Water Research 143 (2018) 367–375

Contents lists available at ScienceDirect

Water Research

journal homepage: www.elsevier.com/locate/watres

Energy consumption in capacitive deionization – Constant current versus constant voltage operation

J.E. Dykstra [a, b, *], S. Porada [b, c], A. van der Wal [a, d], P.M. Biesheuvel [b]

[a] Department of Environmental Technology, Wageningen University, the Netherlands
[b] Wetsus, European Centre of Excellence for Sustainable Water Technology, Leeuwarden, the Netherlands
[c] Soft matter, Fluidics and Interfaces Group, Faculty of Science and Technology, University of Twente, Enschede, the Netherlands
[d] Evides, Rotterdam, the Netherlands

ARTICLE INFO

Article history:
Received 18 November 2017
Received in revised form
24 May 2018
Accepted 15 June 2018
Available online 19 June 2018

Keywords:
Capacitive deionization
Constant current and constant voltage operation
Optimizing salt adsorption
Minimizing energy consumption

ABSTRACT

In the field of Capacitive Deionization (CDI), it has become a common notion that constant current (CC) operation consumes significantly less energy than constant voltage operation (CV). Arguments in support of this claim are that in CC operation the endpoint voltage is reached only at the end of the charging step, and thus the average cell voltage during charging is lower than the endpoint voltage, and that in CC operation we can recover part of the invested energy during discharge. Though these arguments are correct, in the present work based on experiments and theory, we conclude that in operation of a well-defined CDI cycle, this does not lead, for the case we analyze, to the general conclusion that CC operation is more energy efficient. Instead, we find that without energy recovery there is no difference in energy consumption between CC and CV operation. Including 50% energy recovery, we find that indeed CC is more energy efficient, but also in CV much energy can be recovered. Important in the analysis is to precisely define the desalination objective function, such as that per unit total operational time –including both the charge and discharge steps– a certain desalination quantity and water recovery must be achieved. Another point is that also in CV operation energy recovery is possible by discharge at a non-zero cell voltage. To aid the analysis we present a new method of data representation where energy consumption is plotted against desalination. In addition, we propose that one must analyze the full range of combinations of cycle times, voltages and currents, and only compare the best cycles, to be able to conclude which operational mode is optimal for a given desalination objective. We discuss three methods to make this analysis in a rigorous way, two experimental and one combining experiments and theory. We use the last method and present results of this analysis.

© 2018 The Authors. Published by Elsevier Ltd. This is an open access article under the CC BY-NC-ND license (http://creativecommons.org/licenses/by-nc-nd/4.0/).

1. Introduction

Capacitive Deionization (CDI) is a cyclic method of water desalination using porous electrodes, where salt ions are removed during the charging step, temporarily held inside the electrodes, and released again during discharge (Biesheuvel et al., 2017; Hawks et al., 2018). During charging, there is an input of electrical energy, which can partially be recovered during discharge (Długołecki and van der Wal, 2013). Many CDI architectures are possible including the use of flowing electrodes (Hatzell et al., 2015; Rommerskirchen et al., 2015; Doornbusch et al., 2016), chemically modified electrodes (Su and Hatton, 2017), redox-active materials (Lee et al., 2014; Shanbhag et al., 2017), and the addition of ion-exchange membranes (Zhao et al., 2012; Kim and Choi, 2010; Li and Zou, 2011). The most commonly used CDI architecture is the flow-by cell, which employs film electrodes with a spacer channel placed in between, through which the solution flows along the electrodes (Suss et al., 2015). CDI has mainly been applied as a desalination technology for brackish water, while other applications include water softening (Seo et al., 2010) and water reuse for cooling towers (Lee et al., 2006; van Limpt and van der Wal, 2014).

For CDI with film electrodes, an important choice that must be made is whether operation will be at constant voltage (CV) or constant current (CC). There can be various criteria to base this choice on, such as the aim for a constant effluent concentration (CC in Membrane CDI), or a low energy consumption of the process.

* Corresponding author. Department of Environmental Technology, Wageningen University, the Netherlands.
E-mail address: jouke.dykstra@wur.nl (J.E. Dykstra).

https://doi.org/10.1016/j.watres.2018.06.034
0043-1354/© 2018 The Authors. Published by Elsevier Ltd. This is an open access article under the CC BY-NC-ND license (http://creativecommons.org/licenses/by-nc-nd/4.0/).

Note that this choice does not need to be made for steady state operation of CDI with flowing electrodes, but is only necessary for cyclic processes. For carbon electrodes (which we consider from this point onward), in literature it is often reported that CC operation leads to a lower energy consumption than CV operation (Kang et al., 2014, 2016; Choi, 2015; Han et al., 2015; Andelman, 2011; Qu et al., 2016). Kang et al. (2014) show that CC-CDI consumes approximately 30% less energy than CV-CDI for identical electrical charge storage or identical ion removal, without considering energy recovery. Similar differences in energy consumption between CC and CV modes without considering energy recovery were reported by Choi (2015) and by Han et al. (2015). A much higher advantage of CC over CV implied by Andelman (2011) where on theoretical grounds CC was considered to have a twice lower energy use than CV operation. In another study, Qu et al. (2016) show that in CC operation with complete energy recovery, the energy consumption can be as low as 28% of CV operation, i.e., about a factor of three less, and Kang et al. (2016) conclude that energy recovery in CC operation is much more favorable than in CV operation.

Arguments brought forward to explain the lower energy use in CC operation are as follows. First, it is argued that during CC charging the charging voltage is only reached at the end of a charging step, thus on average the cell voltage during charging is lower in CC operation, and thus the electrical energy consumption is lower. In the ideal case, and with the same (endpoint) voltage, this difference amounts to a factor of two. The other argument is that in CC operation it is possible to recover energy which —it is implied— is not possible during CV operation. This is indeed true when CV is operated at zero discharge voltage, as has been the classical approach in CV-CDI. However, also in CV operation, it is possible to discharge at a non-zero cell voltage, and thus energy recovery is possible (Kim et al., 2015).

To compare CC and CV operation, one must precisely define the desalination objective, such that per unit total operational time a certain water recovery and desalination quantity must be achieved. Water recovery, WR, is the ratio of the volume (flow) of desalinated water (diluate), over the volume of feedwater.[1] Desalination quantity will be defined below. For a certain objective function, defined by these the parameters, we must find conditions of operation with lowest energy consumption, which can thereafter be compared for different modes of operation. This is not as straightforward as it may seem: though it is often attempted to compare CC and CV for identical conditions of operation, it is not sufficiently checked whether these conditions result in the same desalination quantity and WR. Choi (2015) compares data for CC and CV operation for identical charging voltages, that is, data are compared where the charging voltage applied in CV operation is the same as the endpoint charging voltage in CC operation. However, for this comparison between any two data points at the same voltage, various other operational properties are different, such as WR, cycle time and salt removal. Kang et al. (2014) compare CV and CC operation as function of the salt adsorption capacity of a cycle. Data points are compared at the same value of salt adsorption capacity, and WR of 50%. However, for each data point used in the comparison, the cycle time (the duration of the full charge/discharge cycle) is different. Thus, Kang et al. (2014) compare the performance of a single cycle, but not the performance per time period of system operation, and therefore the cycle-averaged salt adsorption rates are not equal. Whereas these papers consider flow-by CDI, Qu et al. (2016) perform experiments with flow-through CDI and compare data as function of charge transferred. They show (inset picture Fig. 4 in Qu et al. (2016)) that in their case the amount of charge is close to proportional to salt removal. Furthermore, data were obtained at the same duration of the charging (either CV or CC) and discharge step (CC in all cases). This approach is in line with the proposal of the present paper, which is that one must compare data with the same salt removal rate (when averaged over the full cycle). They show that without energy recovery CC has $\sim$ 35% less energy consumption, and including energy recovery CC has up to a factor of three lower energy consumption. Different to our protocol, Qu et al. (2016) only analyze a first cycle, and not the “dynamic steady state”, but for the longer cycles this should not matter much. Energy consumption was analyzed for flow-by CDI by Zhao et al. (2012) and compared for CC vs CV operation, CDI vs membrane-CDI, and for different salt concentrations. Conclusions in that paper, however, were based on comparing data with different average salt adsorption rates and thus the conclusions do not rigorously follow. Recently, for membrane-CDI, Wang and Lin (2018) conclude that it depends on the desalination objective whether CC is to be favored over CV, or vice-versa.

In order to compare CC and CV operation in a fair manner, one has to make sure that the desalination objective of the cycles subject to comparison is the same. The objective is always defined by two parameters: first, the water recovery, WR,[1] and, second, a measure of the amount of salt removed. The latter can be expressed as the average salt adsorption rate, ASAR, which is based on the molar quantity of salt removed from the diluate stream per unit operational time (Suss et al., 2015). Instead, one can use the average difference in salt concentration between the diluate and feed streams. We call this difference “desalination,” Δc. In this paper we will use Δc, not ASAR, as our measure for the amount of salt removed from the diluate stream in a CDI cycle.

For each operational mode (CV or CC) an infinite number of charging/discharging schemes is possible, which are all defined by different operational parameters. Each scheme results in a desalination cycle with a certain desalination objective and energy consumption. Thus, to reach a certain objective, several operational schemes are possible, and for each scheme the energy consumption can be different. In order to conclude whether CC or CV operation performs better, one has to compare for each operational mode the scheme resulting in the desired objective with the lowest energy consumption. This means that one has to conduct, in principle, an infinite number of experiments. Because the desalination objective, defined by WR and Δc, reached by a certain scheme can only be determined after running the CDI cycle, many experiments must be discarded if we are only interested in one value of WR and Δc to compare CC and CV operation. Instead, we propose that it is better to use all data that are obtained, and thus to compare CC to CV operation for a range of values of WR and Δc. This method would result in a 3D representation of energy use versus WR and Δc. This method, which we refer to as “Experimental 3D”, see Fig. 1, allows for a fair comparison between the operational modes.

Another method, which we refer to as “Experimental 2D”, is based on fixing one of the parameters defining the desalination objective, e.g. WR, at a constant value, and to compare the energy consumption of both operational modes as function of Δc. This means that experiments should be conducted using an operational scheme that results in a pre-defined value of WR, which is not easy, because according to our definition,[1] water recovery is not a parameter that can be imposed directly in an experiment; i.e., it is not an input, but an output of an experiment. Indeed, as we will show, WR can be markedly different from what would be expected

[1] The volume of desalinated water, i.e., the diluate stream, is, in the present work, calculated by multiplying the water flow rate with the duration of the desalination step, which we define as the period when the salt concentration of the effluent of the cell is lower than the concentration of the feed water (Zhao et al., 2013).

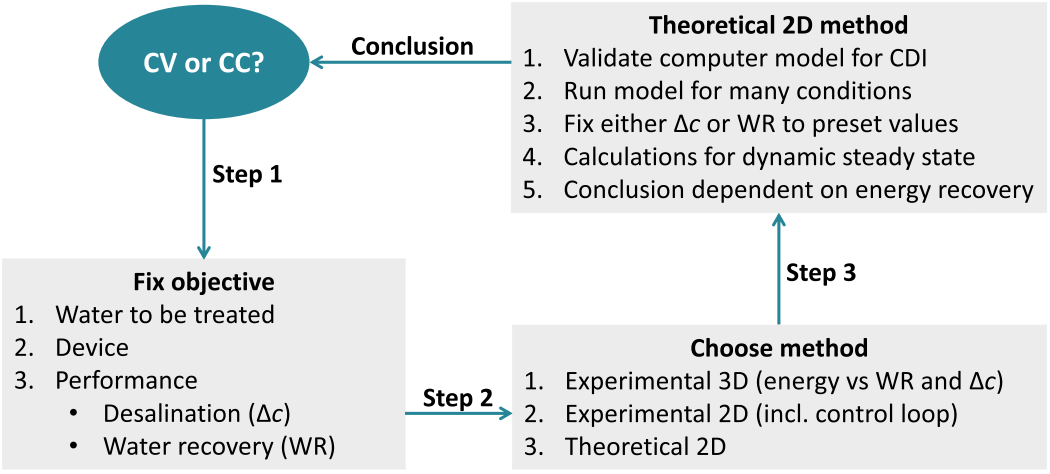

Fig. 1. Schematic overview of our methodology to analyze the suitability of a certain operational mode for water desalination by capacitive deionization (CDI), on the basis of energy consumption.

based on a calculation involving charging and discharging times. Therefore, experiments have to be designed making use of a control loop: a desalination cycle is conducted with several parameters defining a cycle, then the output of a cycle is analyzed and WR calculated, thereafter the parameters are adapted, and this loop is run through until WR reaches the pre-defined value. Also in this case a very large number of experiments are required to find conditions of minimum energy in a plot of energy consumption versus Δc.

Instead of these two experimental methods, we make use of a method which combines experiment and theory, see Fig. 1. This method consists of performing a limited number of experiments to validate a dynamic CDI model (Dykstra et al., 2016a, 2017; Hemmatifar et al., 2015). This model is then used to generate a very large number of calculated outputs of energy use, all at a constant pre-defined value of WR (achieved by a numerical search routine) and these model results are compared in a plot for energy consumption versus desalination, Δc, at fixed values of WR. We refer to this method as "Theoretical 2D".

The objective of the present manuscript is to outline a methodology to assess the energy consumption of a certain operational mode of a certain CDI technology. In the present work, we apply this methodology to the example case of comparing CC and CV operation in CDI. In this method we make use of a computer model of a CDI cell, and run a very large number of calculations with varying values of cycle times, current, voltages, etc., all for the same input and device. In this way, we find for each operational mode (CV or CC) the optimum cycle characteristics and we can control WR exactly, without requiring experiments using a control loop. Optimum values are read off as the lower boundary in a plot of energy versus desalination, Δc (at fixed values of WR). These optimum values (i.e. the lower boundaries) can then be compared to derive information on the merit of CC versus CV operation with respect to energy use, for conditions where the overall performance of the process is the same. The comparison is made at two values of the energy recovery during discharge.

2. Theoretical framework

Theoretical calculations are made using a dynamic CDI model of a single cell, which describes ion electromigration across the spacer channel and through the porous electrode, combined with a suitable EDL-model. For the theoretical equations, we refer the reader to Refs. (Dykstra et al., 2016b). In the flow direction, only a single "sub-cell" is assumed. To describe the EDL structure, for mathematical simplicity, the improved modified Donnan model is used in the calculations, which was compared with the amphoteric Donnan model (Gao et al., 2016; Dykstra et al., 2017; Mubita et al., 2018) and was shown to give similar predictions for salt adsorption, charge and charge efficiency, in the relevant range of salinities of this study, see Supplementary Information (S.I.) Section 1. Values for relevant parameters in this dynamic CDI model are reported in S.I. Section 2.

Calculations are always made for the "dynamic steady state" (DSS) or "limit cycle" by running through at least three cycles, and taking results from the third cycle. Salt adsorption is calculated as the number of moles removed from the diluate stream (based on the difference in inflow and effluent salt concentration), which is also equal to the molar quantity of salt that is added to the concentrate stream. Energy consumption, EC, is equal to the energy input during the charging step, minus the energy that is recovered during the discharge step. Energy input is calculated as the integral of current and cell voltage during the charging step. The energy that is recovered during discharge is the product of current, cell voltage, and an energy recovery factor, integrated over the discharge step. In our calculations, this factor is taken as either 0% or 50%. When this factor is 0%, we do not recover energy, and EC is equal to the energy input. When a factor of 50% is used, energy recovery is included and EC is lower than with a recovery factor of 0%. Energy consumption can be presented in many different ways, such as energy per volume of diluate produced, or energy per unit time. Alternatively, an inverse measure can be used, such as "energy-normalized adsorbed salt" (Hemmatifar et al., 2016). In this paper, we use the metric of energy per molar quantity of salt removed, with unit kJ/mol.

3. Energy consumption as function of desalination - comparing theory and data

Our experimental program is based on the CDI stack described in detail in Dykstra et al. (2016a). The stack consists of four cells, each cell containing two porous activated carbon electrodes (Materials & methods, PACMM^{TM} 203, Irvine, CA, USA). A spacer keeps the electrodes apart and allows for fluid flow. The salt solution is pumped from a vessel with a volume of 10 L, through the cell, thereafter passes a conductivity sensor that records a value each second, and recirculates back to the vessel. The solution in the

vessel is purged with N2 gas to minimize the concentration of dissolved oxygen in solution, and thus, to minimize the occurrence of faradaic reactions that can result in the reduction of desalination performance during the experiments. For more details on the experimental design, we refer the reader to S.I. Section 3. The aim of these experiments was to validate the dynamic CDI model as presented in Section 2.

Experimental results are presented in Fig. 2 as function of desalination, Δc, which is the decrease in salt concentration of the diluate stream compared to the feed stream, averaged over the duration of the desalination step (the time period that the device produces diluate, i.e., that the water leaving the cell has a lower salinity than the feed). For CV operation, Δc increases when we reduce the discharge voltage (at the very right $V_{disch} = 0$ in Fig. 2A,B), while for CC operation moving to the right, data points correspond to higher and higher current densities. As discussed, we do not use these data to directly come to a conclusion about energy in optimized CC or CV cycles, but use these data to validate the dynamic CDI model. As Fig. 2 shows, the fit of model to data is reasonable but certainly not perfect. Though a better fit would have been preferred, still, for the present work, which has the aim to outline a method how to analyze operational modes in CDI, the quality of the fit between the model and data is sufficient. We should note that to fit the model to the data somewhat unrealistic values had to be used for certain parameters in the model, see S.I. Section 2.

For the data shown in Fig. 2, one would perhaps expect that in all cases the water recovery, WR, is 50%, as the charging time was equal to the discharge time, both for CC and CV operation. Indeed, Fig. 3 shows that for most CV data this is the case, but Fig. 3 also shows that for some CV data and all CC data, WR is less than 50%. Thus, although the charging time is equal to the discharge time in all experiments, we find that the adsorption time, which we define as the period when the salt concentration of the effluent is lower than in the feedwater, that this period is considerably shorter than the desorption time, which is the period when the effluent has a higher salt concentration than in the feedwater. This difference in adsorption and desorption time results, with constant flow rate, in WR < 50%. Thus, we cannot simply compare a set of CC and CV experiments, for the reasons outlined before: first, that for a certain operational setting we cannot be sure that we are at the lowest

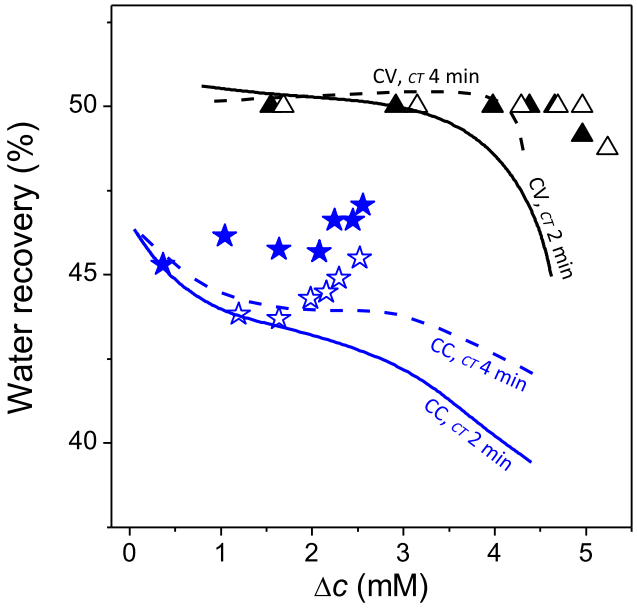

Fig. 3. Water recovery as function of desalination, Δc. Experimental (points) and theoretical results (solid and dashed lines) based on data for which energy consumption is reported in Fig. 2. The duration of a full cycle, CT, is either 2 min (full symbols) or 4 min (open symbols).

energy for a given desalination objective, and second, in most cases the desalination objective is different (both Δc and WR will be different between the CC and CV data points). Therefore, we use a different approach, where the validated CDI model is used to generate many "data-points" of energy use at different values of WR and Δc, for the different operational modes, as will be discussed in the next section.

4. Optimizing desalination performance as function of desalination and WR - comparing constant voltage and constant current operational modes

In Section 3 we validated our dynamic model with experimental data and discussed that we use this model to compare the energy

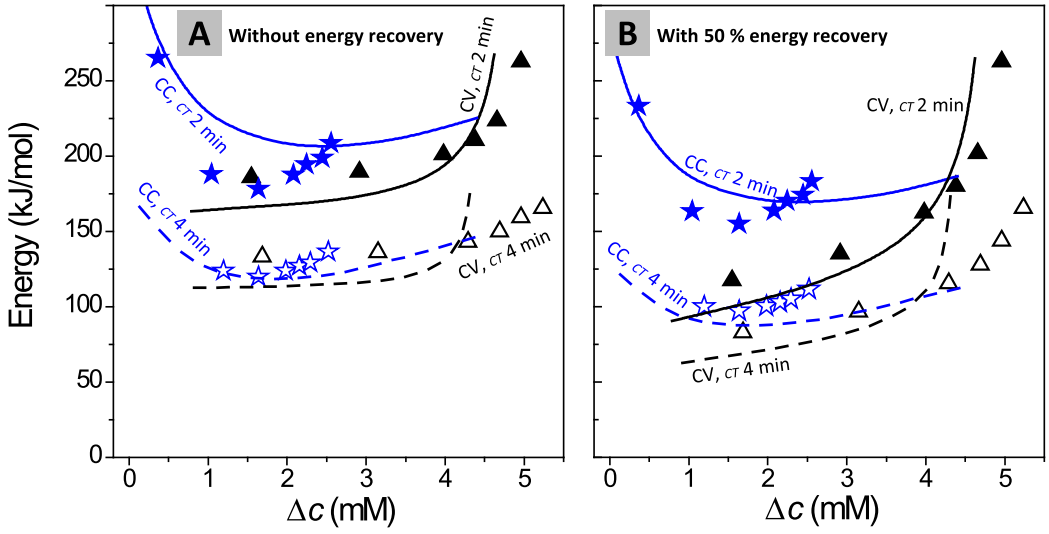

Fig. 2. Energy consumption as function of desalination, Δc. Experimental results based on data (CV: triangles, CC: stars) (as presented in Fig. S2 in S.I. Section 3) and results of theoretical calculations using the dynamic CDI model (solid and dashed lines). A) without energy recovery, and B) with energy recovery. The duration of a full cycle, CT, is either 2 min (full symbols) or 4 min (open symbols). Water recovery is not constant in these experiments.

consumption, EC, of CV and CC operational modes. In the present section we discuss this methodology in more detail, and present the results of the comparison between CV and CC charging in CDI.

To be able to compare CDI cycles for different operational modes, three types of constraints must be the same: the flow rate and composition of the inflowing water, the cell itself (mass of electrodes, dimensions), and the desalination objective. With all of these constraints the same, we can analyze whether one mode of operation has a higher energy consumption than another mode. For a different input, cell, or objective, the conclusion can be quite different. Calculations are based on the same input water and cell design as in the experimental and theoretical program discussed above. Furthermore, the calculations are limited to the following conditions: one level of inflow salinity (single salt solution, NaCl), either CC during charge and discharge, or only CV, thus no mixed modes, and pump rate constant (no variation in pump flow rate such as in "stop flow"-mode (Bouhadana et al., 2011)).

For CV operation, four parameters are required to define a cycle: charging voltage, V_{ch}, discharge voltage, V_{dch}, charging time, t_{ch}, and discharge time, t_{dch}. For CC operation, again four parameters define a cycle: endpoint voltage during charging, V_{up}, charging current, I_{ch}, endpoint voltage during discharge, V_{down}, and discharge current, I_{dch}. For both CV and CC we discussed in Section 3 that, with equal charging and discharge times, water recovery, WR, is not necessarily 50%, and can be different for each calculation. In order to compare CC and CV, one should control the desalination objective, and thus fix WR at a constant value. We make calculations using these four parameters according to the calculation procedure described in Box 1.

Fig. 4 shows calculation results for energy consumption, EC, in CV and CC operational modes for ER 0% (panel A) and ER 50% (panel B), where the latter means that 50% of the energy released during discharge is recovered, and is thus subtracted from the energy input, to calculate EC. Results are shown for WR 50%. As expected, there are many ways to run a cycle to achieve a certain value of Δc, and all have a different energy consumption. Because we are primarily interested in the lowest values of energy for any given Δc, we care most about the lower boundary of the calculation results, which we present in Fig. 5. Fig. 5 shows calculation results not only for WR 50%, but also for WR 40, 60 and 70%, and for each set of calculations we plot the lower boundary of energy consumption. To select the datapoints that mark the boundary out of the full "cloud" of calculation results, a well-defined procedure is required, which we describe in Box 2.

An important assumption to make this procedure work, is that the lower boundary increases concavely upward with Δc.

Now, with lower boundaries plotted in Fig. 5 for different values of WR, with and without 50% energy recovery, we can compare the energy consumption in CC and CV operation. Making this comparison, we see that, without energy recovery, our procedure predicts not much difference in energy consumption between the two operational modes. However, with 50% energy recovery, CC shows a 5–15% lower energy consumption than CV. This moderate difference between energy consumption in CV and CC operation, is in line with recent observations by Wang and Lin (2018) for membrane-CDI.

One may wonder how Fig. 5C and D would be with 100% energy recovery, instead of 50%. In fact, calculations with 100% recovery were made, but resulted in many LB points and only a very limited number of OptLB points. This is because with 100% recovery the calculation procedure predicts that we can increase the upper voltage (CC) and the charging and discharge voltages (CV) to high values, in fact to the maximum values we set, because most of the input energy will be fully recovered anyway. Thus, in case we use an energy recovery factor of 100% it was not possible to obtain a sufficient number of data points to reliably construct the lower boundary in an energy vs. Δc-plot. Furthermore, in our view, a recovery factor of 50% is more realistic than of 100%. A few studies that describe the development and optimization of a back-boost converter for CDI to recover energy during discharge, report a maximum recovery factor of ~ 50% (Alkuran and Orabi, 2008; Kang et al., 2016), although other studies also report an efficiency ~ 80% (Pern et al., 2012) and even ~ 100% (Prieto et al., 2014).

For the optimal points as plotted in Fig. 5, we listed in S.I. Section 4 all values for V_{ch}, V_{dch}, t_{ch} and t_{dch} (CV) and I_{ch}, I_{dch}, t_{ch} and V_{down} (CC). Interestingly, we find that, for CV, cycles with optimum desalination performance have a discharge voltage of $V_{disch} = 0.3$ V or higher, which is in line with results reported by Kim et al. (2015), where it was concluded that increasing the discharge voltage from 0 V to 0.3 V results in a higher charge efficiency. For CC operation we find a similar result, but only for calculations based on 50% energy recovery. Without recovery, there is no clear dependence on the endpoint voltage during discharge.

Finally, we analyze why, without energy recovery, our procedure predicts not much difference in energy consumption between the two modes of operation, and why, with 50% energy recovery, CC consumes less energy than CV. To that end, for both operational modes we make a detailed calculation of the various contributions to the energy, see Fig. 6. We compare here a CC cycle with a CV cycle, and both cycles have the same Δc and WR, and without energy recovery, have almost the same energy consumption (without

Box 1
Calculation procedure

1 Of the four parameters that define a cycle we make a "sweep" over the first three parameters (for CV: V_{ch}, V_{dch}, and t_{ch}; for CC: I_{ch}, V_{up}, and V_{down}) in a large window of suitable values. In Table S2 we list for each parameter which domain is scanned, and the interval between each value.
2 Based on the desired WR, we calculate a guess value for the fourth parameter (for CV: t_{dch}; for CC: I_{dch}). For CV, we use $t_{dch} = t_{ch}\left(\frac{1}{WR_{desired}} - 1\right)$, and for CC, we use $I_{dch} = \frac{WR_{desired} \cdot I_{ch}}{1-WR_{desired}}$.
3 For each combination of parameter values we run the CDI model for three cycles consecutively. Based on the output (current, effluent concentration) of the last cycle, for which we reached a dynamic steady state, we calculate the realized WR, energy consumption (for ER 0% and ER 50%) and Δc.
4 Using a numerical routine, we repeat step 3 with t_{dch} (CV) or I_{dch} (CC) as variables to minimize the error given by error $= (WR_{desired} - WR_{realized})^2$.
5 When the error has become small enough, the calculation was considered successful. For CV, this means that, for given V_{ch}, V_{dch}, and t_{ch}, we have found a value for t_{dch} that characterizes a desalination cycle with $WR_{desired}$; and for CC, this means that, for given I_{ch}, V_{up}, and V_{down}, we found a value for I_{dch}. For this desalination cycle, we plot values for energy consumption (for ER 0% and ER 50%) as function of Δc in Fig. 4.
6 We repeat this procedure for all combinations of parameters listed in Table S2. For some combinations of parameters there was no solution, and then no datapoints are plotted in Fig. 4.

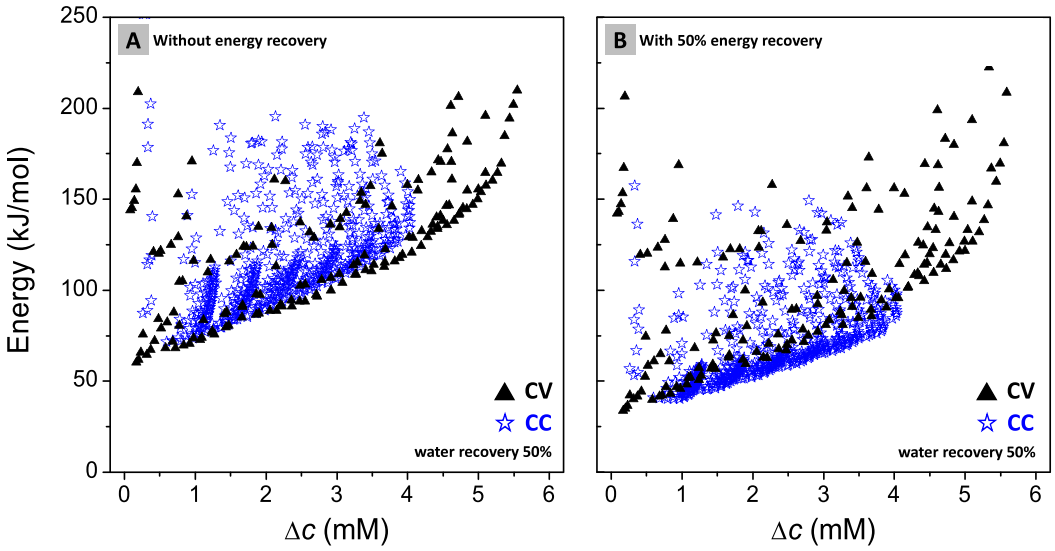

Fig. 4. Energy consumption as function of desalination, Δc, A) without and B) with 50% energy recovery, based on a large set of calculations to find the lower boundary for CC and CV operation (water recovery 50%).

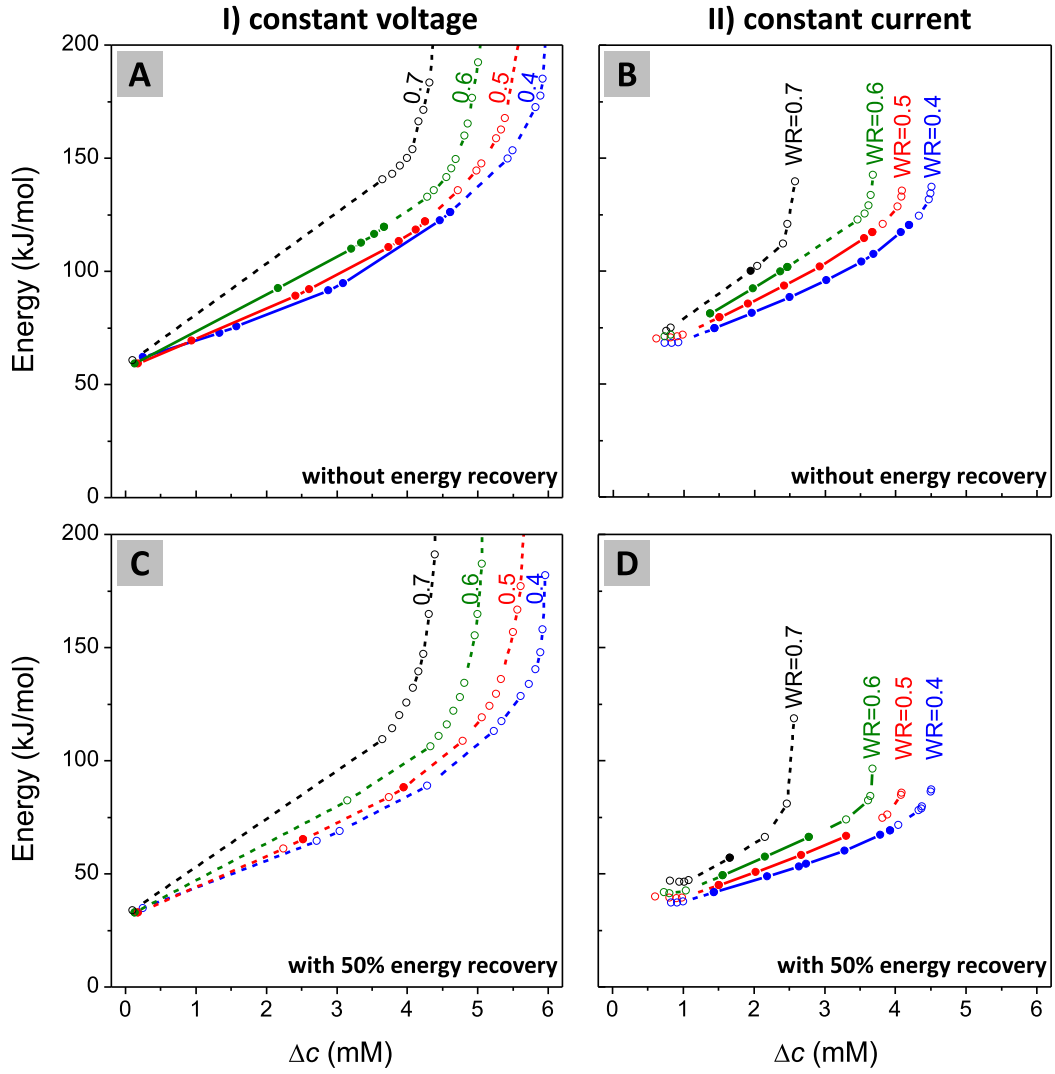

Fig. 5. Minimum energy consumption as function of desalination, Δc, and water recovery, WR. Solid datapoints, connected by solid lines, are OptLB points, whereas open datapoints, connected by dashed lines, are LB points, points located at the boundaries of our tested parameter domain. Panel A and C show results for CV and B and D for CC, without (A and B) and with (C and D) 50% energy recovery.

Box 2
Selecting datapoints at the lower boundary in an EC-Δ*c* plot

1 We select the datapoint with lowest EC, which will be the starting point marking the lower boundary, with coordinates (x_{start},y_{start}), where x refers to Δc and y to WR.
2 Now, the procedure selects the next point – positioned to the right of the starting point – that marks the lower boundary. Therefore, for each datapoint i with $x_i > x_{start}$ the slope is calculated using $a_i = \frac{x_i - x_{start}}{y_i - y_{start}}$.
3 The datapoint with the lowest slope is selected as the next point marking the lower boundary.
4 We check whether this point is one of the inner points in the calculation domain defined in Table S2, and in that case we refer to it as an OptLB point (solid symbols in Fig. 5). Else, the point is at the boundaries we set for the parameter values, and it is likely that, if the boundaries would have been set differently, a datapoint with lower energy consumption would have been found. We refer to this point as a LB point (open symbols in Fig. 5).
5 We repeat this procedure from step 2 onwards, and replace subscript "start" by "prev" with values for coordinates (x_{prev},y_{prev}) being (x_i,y_i) found in step 3. The procedure is terminated when there is no longer a datapoint for which $x_i > x_{prev}$.

energy recovery: CV: EC= 89.2 kJ/mol; CC: EC = 93.4 kJ/mol; with 50% energy recovery: CV: EC = 65.6 kJ/mol; CC: EC = 56.3 kJ/mol). Both cycles are at the lower boundary in Fig. 5. For both modes of operation, we study the energy in the separate elements of the cell: the EDLs (Donnan and Stern potential), ionic resistances in spacer and macropores, and electronic resistances in cables and current collectors. The equations required for this analysis are described in S.I. Section 5.

Fig. 6 first of all shows the energy stored in the Stern and Donnan layers in the electrodes during charging. Note how for CV operation, the energy stored in the Stern layer is much lower than for CC operation (CV: 56.3 kJ/mol; CC: 68.2 kJ/mol). During discharge, the energy stored in the Stern layer is released again, but for the Donnan layer, not all energy that was stored is again released, which can be explained as follows. During charging, the Donnan layer is charged while the salt concentration in the macropores is low, resulting in a high Donnan potential between macropores and micropores. Instead, during discharge, the salt concentration in the macropores is much higher, and thus, the Donnan potential is lower. Consequently, the energy released from the Donnan layer during discharge is less than the energy required to charge the layer.

Fig. 6 also shows that, both during charging and discharge, energy is dissipated due to the ionic resistances in the spacer and electrodes (mA), and due to electronic resistances in cables and current collectors (EER). Comparing CV and CC, we observe that the energy dissipation due to resistances is higher in CV than in CC, both during charging and discharge, which can probably be explained by the high currents directly at the start of a CV charging step and, consequently, by the low salt concentrations in the spacer and electrodes, resulting in a high resistance.

Although the energy dissipation due to resistances is much higher in CV mode than in CC mode, we find that the total energy input (sum of all bars for "end of charging"; equal to energy consumption in case of 0% energy recovery) is slightly lower for CV than for CC. As Fig. 5 shows, this is because, for CV, the Stern layer in the EDL needs to be charged less to reach the required Δc and WR (56 kJ/mol for CV vs. 68 kJ/mol for CC).

Finally, we like to note that, as Figs. 2 and 3 showed, the CDI transport model did not perfectly describe experimental data for all values of Δc. The level of fit of the model to the data of course directly impacts the correctness of our observations, such as for the relative level of energy consumption in CC and CV operation. Thus, to come to more solid conclusions, it is useful to find a CDI model (and its parameter settings) which describes data more precisely.

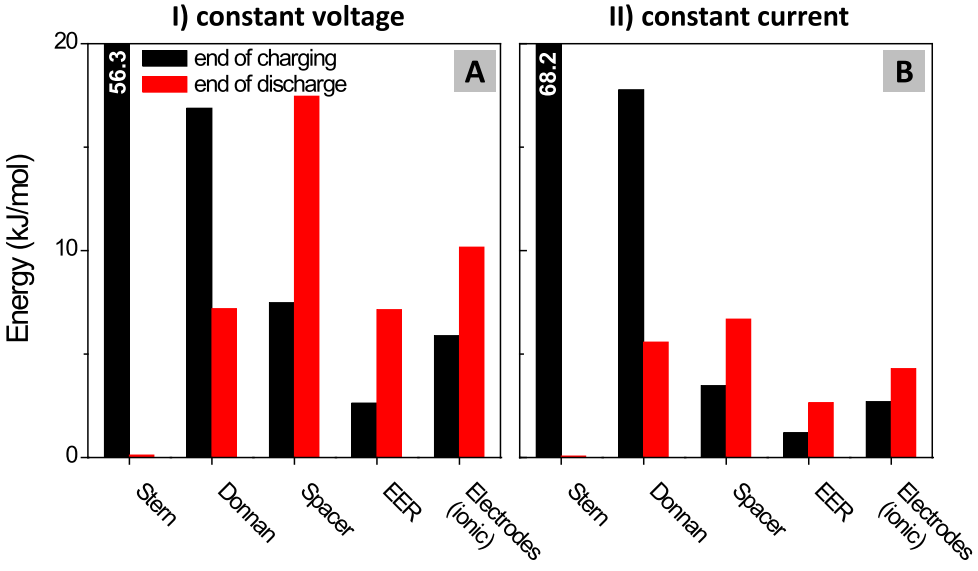

Fig. 6. Contributions to energy at the end of charging and at the end of discharge of a CDI cell, for A) constant voltage and B) constant current operation (for both panels: desalination Δc = 2.42 mM, water recovery WR = 50%). Energy stored in EDLs (Donnan and Stern layer) can (partly) be recovered during discharge. During charging and discharge, energy is dissipated by ionic resistances in spacer and electrodes (mA), and by electronic resistances in cables and current collectors (EER). Parameter values that define the desalination cycle are for A) given in Table S3, and for B) given in Table S5 (WR = 0.5, Δc = 2.42 mM).

Nevertheless, for the objective of our work, which is to present a method of CDI cycle analysis and energy use, the CDI model used has been an essential tool.

5. Conclusions

In this manuscript, we presented a methodology to assess the energy consumption of a certain operational mode of CDI operation, and we apply this methodology to compare constant current and constant voltage charging in CDI: constant voltage (CV) and constant current (CC). In this methodology, we use a validated CDI model that can be used in both operational modes. We define several constraints and parameters describing desalination cycles for both CC and CV, and we calculate for a range of parameter combinations the energy consumption (with and without 50% energy recovery during discharge), water recovery, WR, and the decrease in salt concentration of the diluate (averaged over the salt adsorption period Δc). Thereafter, we plot the lowest values of energy consumption as function of Δc and WR. This robust methodology showed that, in our example calculation, without energy recovery, the lowest values of energy consumption of CV and CC operation are approximately the same. If 50% of the energy released during discharge can be recovered and reused in CDI, CC has a somewhat lower energy consumption than CV.

The methodology can be extended to analyze mixed modes of operation (e.g. CC charging and CV discharge, or vice-versa), and operation with a water flow rate that has different values during the cycle, which can be useful to increase WR. Furthermore, the methodology can be used to find parameter combinations for optimum desalination performance in membrane-CDI, and in other cell designs. It must be noted that the CDI transport model we make use of in our methodology, did not perfectly describe experimental data for all values of Δc. If the aim is to find exact values for parameter settings of CDI operation, to reach the lowest energy consumption at a certain desalination objective, then a better fit between data and theory, and consequently a better model, is required.

Acknowledgement

This work was performed in the cooperation framework of Wetsus, European Centre of Excellence for Sustainable Water Technology (www.wetsus.eu). Wetsus is co-funded by the Dutch Ministry of Economic Affairs and Climate Policy and Ministry of Infrastructure and Water Management, the Province of Fryslân, and the Northern Netherlands Provinces. The authors like to thank the participants of the research theme Capacitive Deionization for fruitful discussions and financial support. S.P. acknowledges financial support by the Dutch Technology Foundation STW, which is part of the Netherlands Organisation for Scientific Research (NWO), and which is partly funded by the Ministry of Economic Affairs (VENI grant no 15071).

Appendix A. Supplementary data

Supplementary data related to this article can be found at https://doi.org/10.1016/j.watres.2018.06.034.

References

Alkuran, M., Orabi, M., 2008. Utilization of a buck boost converter and the method of segmented capacitors in a CDI water purification system. In: 2008 12th International Middle-east Power System Conference, pp. 470–474.
Andelman, M., 2011. Flow through capacitor basics. Separ. Purif. Technol. 80, 262–269.
Biesheuvel, P.M., et al., 2017. Capacitive Deionization – Defining a Class of Desalination Technologies arXiv:1709.05925.
Bouhadana, Y., Ben-Tzion, M., Soffer, A., Aurbach, D., 2011. A control system for operating and investigating reactors: the demonstration of parasitic reactions in the water desalination by capacitive de-ionization. Desalination 268, 253–261.
Choi, J.-H., 2015. Comparison of constant voltage (CV) and constant current (CC) operation in the membrane capacitive deionisation process. Desalination Water Treat. 56, 921–928.
Długołecki, P., van der Wal, A., 2013. Energy recovery in membrane capacitive deionization. Environ. Sci. Technol. 47, 4904–4910.
Doornbusch, G.J., Dykstra, J.E., Biesheuvel, P.M., Suss, M.E., 2016. Fluidized bed electrodes with high carbon loading for water desalination by capacitive deionization. J. Mater. Chem. A 4, 3642–3647.
Dykstra, J.E., Dijkstra, J., Van der Wal, A., Hamelers, H.V.M., Porada, S., 2016a. On-line method to study dynamics of ion adsorption from mixtures of salts in capacitive deionization. Desalination 390, 47–52.
Dykstra, J.E., Keesman, K.J., Biesheuvel, P.M., van der Wal, A., 2017. Theory of pH changes in water desalination by capacitive deionization. Water Res. 119, 178–186.
Dykstra, J.E., Zhao, R., Biesheuvel, P.M., Van der Wal, A., 2016b. Resistance identification and rational process design in Capacitive Deionization. Water Res. 88, 358–370.
Gao, X., Porada, S., Omosebi, A., Liu, K., Biesheuvel, P.M., Landon, J., 2016. Complementary surface charge for enhanced capacitive deionization. Water Res. 92, 275–282.
Han, L., Karthikeyan, K.G., Gregory, K.B., 2015. Energy consumption and recovery in capacitive deionization using nanoporous activated carbon electrodes. J. Electrochem. Soc. 162, E282–E288.
Hatzell, K.B., Hatzell, M.C., Cook, K.M., Boota, M., Housel, G.M., McBride, A., Kumbur, E.C., Gogotsi, Y., 2015. Effect of oxidation of carbon material on suspension electrodes for flow electrode capacitive deionization. Environ. Sci. Technol. 49, 3040–3047.
Hawks, S.A., Ramachandran, A., Campbell, P.G., Suss, M.E., Biesheuvel, P.M., Santiago, J.G., Stadermann, M., 2018. Performance Metrics for the Objective Assessment of Capacitive Deionization Systems arXiv:1805.03247.
Hemmatifar, A., Palko, J.W., Stadermann, M., Santiago, J.G., 2016. Energy breakdown in capacitive deionization. Water Res. 104, 303–311.
Hemmatifar, A., Stadermann, M., Santiago, J.G., 2015. Two-dimensional porous electrode model for capacitive deionization. J. Phys. Chem. C 119, 24681–24694.
Kang, J., Kim, T., Jo, K., Yoon, J., 2014. Comparison of salt adsorption capacity and energy consumption between constant current and constant voltage operation in capacitive deionization. Desalination 352, 52–57.
Kang, J., Kim, T., Shin, H., Lee, J., Ha, J.-I., Yoon, J., 2016. Direct energy recovery system for membrane capacitive deionization. Desalination 398, 144–150.
Kim, T., Dykstra, J.E., Porada, S., van der Wal, A., Yoon, J., Biesheuvel, P.M., 2015. Enhanced charge efficiency and reduced energy use in capacitive deionization by increasing the discharge voltage. J. Colloid Interface Sci. 446, 317–326.
Kim, Y.J., Choi, J.H., 2010. Improvement of desalination efficiency in capacitive deionization using a carbon electrode coated with an ion-exchange polymer. Water Res. 44, 990–996.
Lee, J., Kim, S., Kim, C., Yoon, J., 2014. Hybrid capacitive deionization to enhance the desalination performance of capacitive techniques. Energy Environ. Sci. 7, 3683–3689.
Lee, J.B., Park, K.K., Eum, H.M., Lee, C.W., 2006. Desalination of a thermal power plant wastewater by membrane capacitive deionization. Desalination 196, 125–134.
Li, H.B., Zou, L., 2011. Ion-exchange membrane capacitive deionization: a new strategy for brackish water desalination. Desalination 275, 62–66.
Mubita, T.M., Porada, S., Biesheuvel, P.M., van der Wal, A., Dykstra, J.E., 2018. Capacitive deionization with wire-shaped electrodes. Electrochim. Acta 270, 165–173.
Pern, A.M., Norniella, J.G., Mart, J.A., Juan, D., 2012. Up – down converter for energy recovery in a CDI desalination system. IEEE Trans. Power Electron. 27, 3257–3265.
Prieto, M.A.J., Villegas, P.J., Nu, F., 2014. New control strategy of an up – down converter for energy recovery in a CDI desalination system. IEEE Trans. Power Electron. 29, 3573–3581.
Qu, Y., Campbell, P.G., Gu, L., Knipe, J.M., Dzenitis, E., Santiago, J.G., Stadermann, M., 2016. Energy consumption analysis of constant voltage and constant current operations in capacitive deionization. Desalination 400, 18–24.
Rommerskirchen, A., Gendel, Y., Wessling, M., 2015. Single module flow-electrode capacitive deionization for continuous water desalination. Electrochem. Commun. 60, 34–37.
Seo, S.J., Jeon, H., Lee, J.K., Kim, G.Y., Park, D., Nojima, H., Lee, J., Moon, S.H., 2010. Investigation on removal of hardness ions by capacitive deionization (CDI) for water softening applications. Water Res. 44, 2267–2275.
Shanbhag, S., Bootwala, Y., Whitacre, J.F., Mauter, M.S., 2017. Ion transport and competition effects on $NaTi_2(PO)_4$ and $Na_4Mn_9O_{18}$ selective insertion electrode performance. Langmuir 2.
Su, X., Hatton, T.A., 2017. Redox-electrodes for selective electrochemical separations. Adv. Colloid Interface Sci. 244, 6–20.
Suss, M.E., Porada, S., Sun, X., Biesheuvel, P.M., Yoon, J., Presser, V., 2015. Water desalination via capacitive deionization: what is it and what can we expect from it? Energy Environ. Sci. 8, 2296–2319.
van Limpt, B., van der Wal, A., 2014. Water and chemical savings in cooling towers

by using membrane capacitive deionization. Desalination 342, 148–155.
Wang, L., Lin, S., 2018. Membrane capacitive deionization with constant current vs constant voltage charging: which is better? Environ. Sci. Technol. 52, 4051–4060.
Zhao, R., Biesheuvel, P.M., van der Wal, A., 2012. Energy consumption and constant current operation in membrane capacitive deionization. Energy Environ. Sci. 5, 9520–9527.
Zhao, R., Porada, S., Biesheuvel, P.M., van der Wal, A., 2013. Energy consumption in membrane capacitive deionization for different water recoveries and flow rates, and comparison with reverse osmosis. Desalination 330, 35–41.